Central symmetry in two-dimensional lattices and quantum information transmission

Zhao-Ming Wang[1,2,*] and Lian-Ao Wu[2,3,†]

[1]*Department of Physics, Ocean University of China, Qingdao 266100, China*

[2]*Department of Theoretical Physics and History of Science, The Basque Country University (EHU/UPV), 48008 Bilbao, Spain*

[3]*IKERBASQUE, Basque Foundation for Science, 48011 Bilbao, Spain*

(Received 12 April 2013; published 26 June 2013)

We present a method to numerically calculate the dynamics driven by arbitrary Hamiltonians, in particular those with symmetry. The method enables us to study quantum state and entanglement transmission through a uniformly coupled two-dimensional square lattice with *XY*-type interaction. Significantly, we find that the central symmetry between sending and receiving nodes plays a crucial role in attaining maximal fidelity and entanglement transmission. In other words, the quality of a two-dimensional transmission is determined by the geometry of the nodes involved.

DOI: 10.1103/PhysRevA.87.064301 PACS number(s): 03.67.Hk, 75.10.Jm

I. INTRODUCTION

Transmission of quantum states from one location to another is often required in quantum information processing. One of the natural mediators for such a task is a spin chain [1–10]. The motivation for using an unmodulated Heisenberg spin chain dates back to Bose's work [1]. Later literature shows that a quantum state can be transferred perfectly by properly preengineering the couplings between nearest-neighbor sites [2].

Antiferromagnetic *XY* models for quantum state transmission (QST) have been paid special attention (see, e.g., [3,9]) because of their simplicity and symmetry. High-fidelity QST can be obtained by encoding multiple-spin quantum states [5] in these models. A physical explanation for obtaining such high fidelity is given in recent literature [10–12]. These publications also present a method for the numerical determination of *good* initial states which result in high-fidelity state transmission or even perfect state transfer [2].

However, most previous QST literature concerns one-dimensional spin chains, although QSTs on two- and three-dimensional lattices have also received attention sporadically [13–16]. In Ref. [13] analytic models that can perfectly transfer arbitrary quantum states in two- and three-dimensional interacting bosonic and fermionic networks are found by properly engineering the couplings. In Ref. [14] QSTs through a two-dimensional regular spin lattice with nonuniform coupling are analyzed and high fidelity QST is obtained. QSTs in a two-dimensional hexagonal lattice and a three-dimensional lattice are investigated in Ref. [15]. Quantum state and entanglement transmission through a two-dimensional spin network with periodic boundary conditions may have an analytical solution and has been investigated recently [16]. Entanglement properties in a two-dimensional triangular lattice with impurities are investigated in Refs. [17] and [18], where Ising and *XY*-type interactions are considered, respectively. Experimentally it is hard to realize the required nonuniform couplings between sites, whereas uniform couplings between spin sites are much more feasible with state-of-the-art technologies.

Most spin models do not have analytical solutions, in particular higher-dimensional ones, for instance, the two-dimensional nearest-neighbor *XY* model with uniform couplings. Unlike analytical approaches, this paper presents a method to exactly and numerically calculate single-excitation dynamics of a two-dimensional nearest-neighbor *XY* model with uniform couplings. The method allows us to study quantum state and entanglement transmission driven by this model.

This paper is organized as follows. In Sec. II we present the two-dimensional *XY* model Hamiltonian and introduce a numerical method to calculate the system dynamics. In Sec. III we show our results and analyze them. We conclude in Sec. IV.

II. THE MODEL AND THE CALCULATION OF THE FIDELITY

Consider the spin dynamics in a two-dimensional square lattice driven by the nearest-neighbor Heisenberg *XY* model,

$$H = -J\Bigg(\sum_{i=1}^{N-1}\sum_{j=1}^{N} X_{i,j}X_{i+1,j} + Y_{i,j}Y_{i+1,j} + \sum_{i=1}^{N}\sum_{j=1}^{N-1} X_{i,j}X_{i,j+1} + Y_{i,j}Y_{i,j+1}\Bigg), \tag{1}$$

where J is the coupling constant. The indices (i,j) label the locations of sites, where $i,j \in 1,2,\ldots,N$.

Figure 1 shows schematically the coupling patterns of the model Hamiltonian. We consider a natural configuration of the lattices with open boundary. $X_{i,j}$, $Y_{i,j}$, and $Z_{i,j}$ denote the Pauli operators acting on the spin at site (i,j). The z component of the total spin or *the excitation number* is conserved,

$$\left[H, \sum_{i,j=1}^{N} Z_{i,j}\right] = 0. \tag{2}$$

A quantum state will time evolve within a given excitation subspace. In particular, the quantum state in the zero-excitation subspace, where all spins are down, does not time evolve. Therefore, an arbitrary state $\alpha|0\rangle + \beta|1\rangle$ will be transferred perfectly, as long as the state $|1\rangle$ can completely pass through the lattice. We can restrict ourselves to the one-excitation

*mingmoon78@126.com

†lianao_wu@ehu.es

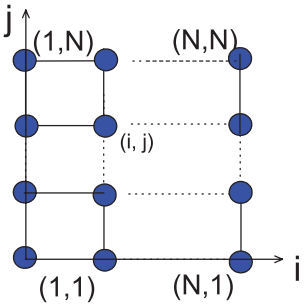

FIG. 1. (Color online) Two-dimensional square lattice with sites labeled by (i,j), where $i,j \in (1,\ldots,N)$.

subspace spanned by N^2 states $|i,j\rangle$, which denotes that the spin at site (i,j) is up ($|1\rangle$) while the other spins are down ($|0\rangle$).

In the one-excitation subspace, we can diagonalize the Hamiltonian H with the matrix W such that $H_d = W^\dagger H W$. The evolution operators can therefore be expressed by

$$U(t) = W \exp[-itH_d]W^\dagger. \tag{3}$$

With time evolution, the excitation at site (i,j) begins to spread outward, and at a later time there is typically a nonzero probability of finding any of the spins in an excitation state. We denote the reduced density matrix at site (k,l) as $\rho(t)$ and the fidelity, measuring the probability of this excitation, is therefore $F = \sqrt{\langle\phi(0)|\,\rho(t)\,|\phi(0)\rangle}$. When $F = 1$, state transfer from site (i,j) to (k,l) is perfect. We now calculate the fidelity, in particular its dependence on the locations of the sender and receiver.

III. RESULTS AND DISCUSSION

We consider that the single excitation $|1\rangle$ is initially at site (i,j). The excitation then time evolves and is distributed to other sites due to the interaction among spins. For a one-dimensional chain, the excitation propagates only along the chain, whereas for the two-dimensional lattice, it is allowed to travel through different routes on the two-dimensional network. We will explore numerically, for the given geometry in Fig. 1, the sending and corresponding receiving locations that are in favor of high-fidelity state transmission.

Figure 2 plots the maximum fidelity $F_{\max}$ versus the site coordinates (i,j) when $N = 13$ in a time interval $[0,4000]$. The figure shows that for a given sending node, the receiving nodes with highest-fidelity $F_{\max}$ are located correspondingly. In Fig. 2(a), the sending nod is at a corner $(1,1)$. Good fidelity can be obtained for nodes along the diagonal. The maximum fidelity $F_{\max}$ occurs at the other corner of the diagonal $(13,13)$, which is symmetric with respect to the center of the lattice. In general, it is interesting to find that, given a sending node (i,j), $F_{\max}$ always occurs at $(N+1-i, N+1-j)$, center-symmetric to the node (i,j). Figure 2 illustrates this interesting observation. For instance, when the excitation is initially at site $(1,7)$, $F_{\max}$ is at the symmetric site $(13,7)$. If we put the excitation at the center $(7,7)$ as shown in Fig. 2(d), it will spread in all directions and $F_{\max} = 0.41$ occurs at the four corners, and is much lower than in the other three cases. This

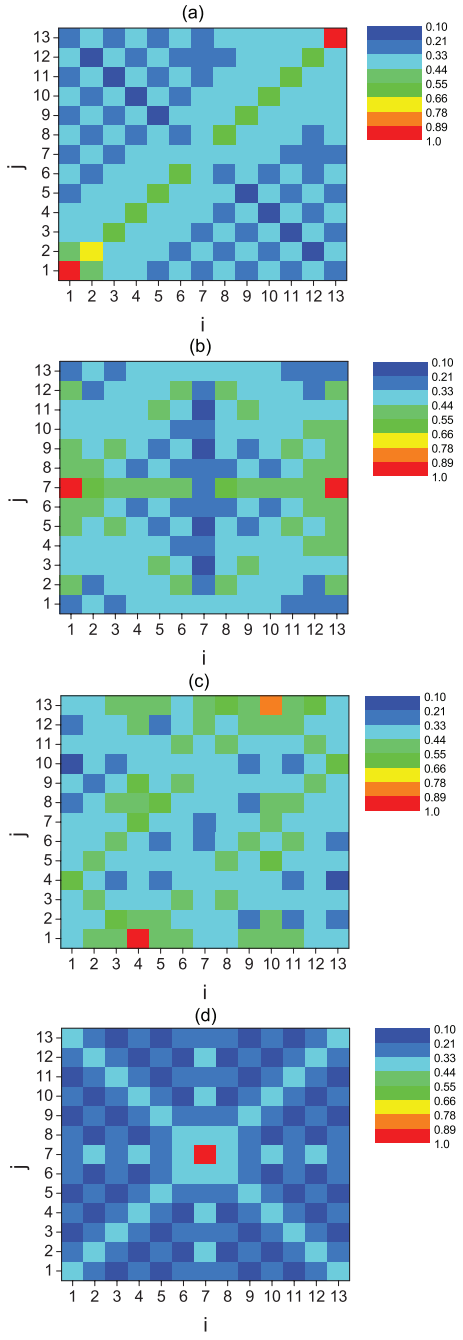

FIG. 2. (Color online) The maximum fidelity at sites (i,j). Initial excitation at (a) corner site $(1,1)$, (b) middle site $(1,7)$, (c) site $(4,1)$, and (d) site $(7,7)$. $N = 13$. $F_{\max}$ is obtained in a time interval $[0,4000]$, which is used throughout the paper.

shows that central symmetry plays a very important role in getting high-fidelity two-dimensional state transmission.

Physically, the initial *wave packet* $|1\rangle$ at the sending node propagates on the lattice plane and spreads in all directions. It will be reflected at boundaries, bounce back and forth, and travel on the lattice plane. Because it is dispersing during the propagation, the wave packet will interfere with itself [19]. The complex dynamical process results in constructive interferences at certain time moments when the fidelity peaks. A wave packet bounces back and forth many times among the four

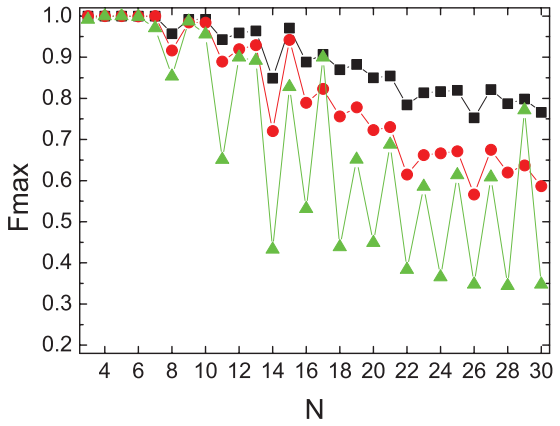

FIG. 3. (Color online) Comparison of the maximum fidelity $F_{\max}$ as a function of the number of sites N for one-dimensional chains and the edge length N of two-dimensional lattices. The circular (red) dots correspond to $F_{\max}$ versus N for the pair pattern $(1,1)$ and (N,N) and the square (black) dots to that for the one-dimensional chain. The triangular (green) dots are $F_{\max}$ of the transmission from site $(1,N/2)$ to $(N,N/2+1)$ when N is even, and from $(1,(N+1)/2)$ to $(N,(N+1)/2)$ when N is odd.

boundaries, and the highest fidelity emerges at the sites that the wave packet passes through with highest probability. The pair pattern (i, j) and $(N+1-i, N+1-j)$, in particular $(1, 1)$ and (N, N), exemplifies the observation.

So far, we have presented the analysis for the case when length $N = 13$. We now analyze the length dependence of the fidelity. Figure 3 plots the maximum fidelity $F_{\max}$ as a function of N, where N is either the number of sites of an XY chain or the edge length of our two-dimensional lattice network. The square (black) dots are for the one-dimensional chain and the circular (red) dots correspond to the pair pattern $(1,1)$ and (N,N). The triangular (green) dots show $F_{\max}$ of the transmission from site $(1,N/2)$ to $(N,N/2+1)$ when N is even, and from $(1,(N+1)/2)$ to $(N,(N+1)/2)$ when N is odd. Interestingly, the former $F_{\max}$ is higher than the latter, except for $N = 17,29$. There are other noticeable features in this figure. For smaller N $(= 3,4,5,6)$, state transmissions are almost perfect for all three cases. The maximal fidelity $F_{\max}$ decreases with N. For a given N, $F_{\max}$ in two-dimensional lattices is lower than that in the one-dimensional chain, and the difference becomes larger with N. This is as expected because a two-dimensional state transmission, in particular the pair pattern $(1,1)$ and (N,N), propagates through N^2 sites whereas a one-dimensional state transmission propagates only through N sites. The more sites are involved, the harder it is for the constructive interference to occur. This seems to imply that a two-dimensional state transmission from $(1,1)$ to (N,N) should be *equivalent* to one-dimensional state transmission with N^2 sites. However, in practice they do not behave similarly because the two-dimensional transmission has less *resistance* due to the involvement of many more routes. We also notice that there is an even-odd oscillation of $F_{\max}$ and odd numbers of sites are favorable. This is a typical finite-size effect [20].

Entanglement is at the center of quantum information processing, and is a resource that allows quantum processes to outperform their classical counterparts for communication and computation cryptography. Fortunately, our method also permits us to study the entanglement transfer in our two-dimensional network. Consider the initial entanglement $\alpha|01\rangle + \beta|10\rangle$ created between sites (i,j) and (k,l). The corresponding initial state of the whole system is

$$|\Phi(0)\rangle = \alpha|i,j\rangle + \beta|k,l\rangle. \tag{4}$$

Now with time evolution the entanglement spreads to sites (i',j') and (k',l'). The state of the whole system at time t is therefore

$$|\Phi(t)\rangle = \sum_{p,q=1}^{N} g_{p,q}(t)|p,q\rangle, \tag{5}$$

where (p,q) represents an arbitrary location of sites and $g_{p,q}(t) = \alpha U_{(p,q),(i,j)}(t) + \beta U_{(p,q),(k,l)}(t)$. The reduced density matrix of the pairs (i',j') and (k',l') is obtained by tracing over the rest of the sites. We use concurrence as an entanglement measure for quantifying the amount of entanglement shared between the spin pairs, which simply reads

$$C_{(i',j'),(k',l')} = 2|g_{i',j'}||g_{k',l'}| \tag{6}$$

for our specific case.

Initially we prepare the maximal entangled state $\alpha = \beta = 1/\sqrt{2}$ between sites $(1,1)$ and $(1,N)$, and calculate the time evolution of the concurrence $C_{(N,1),(N,N)}$. As a comparison, we also prepare the initial entanglement between sites $(1,N/2)$ and $(1,N/2+1)$ when N is even, and between $(1,(N-1)/2)$ and $(1,(N+1)/2)$ when N is odd. We then calculate $C_{(N,N/2),(N,N/2+1)}$ and $C_{(N,(N-1)/2),(N,(N+1)/2)}$ for even and odd N, respectively. Notice that we retain the central symmetry between the sending sites and receiving sites in the process.

Figure 4 plots the maximum concurrence $C_{\max}$ as a function of the edge length N for both cases. The circular (square) dots stand for the maxima $C_{\max}$ of $C_{(N,1),(N,N)}$ ($C_{(N,N/2),(N,N/2+1)}$ or $C_{(N,(N-1)/2)),(N,(N+1)/2)}$) versus N. $C_{\max}$ remains the same for $N = 3,4,5,6$, and then drops and shows similar oscillations as $F_{\max}$ in Fig. 3. For small systems, the entanglement can be perfectly transferred. When $N > 7$, $C_{\max}$ decreases

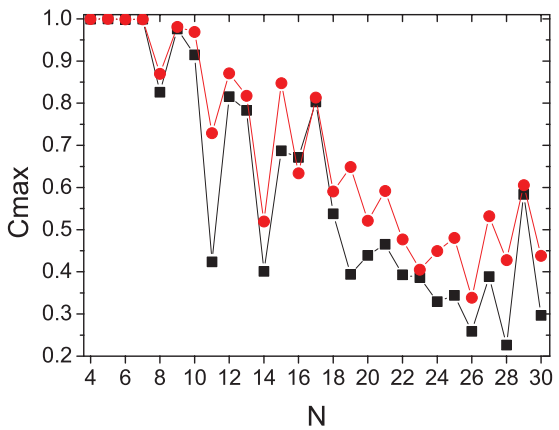

FIG. 4. (Color online) The maximum concurrence $C_{\max}$ as a function of edge length N. The circular (square) dots are the maxima $C_{\max}$ of $C_{(N,1),(N,N)}$ ($C_{(N,N/2),(N,N/2+1)}$ or $C_{(N,(N-1)/2),(N,(N+1)/2)}$) versus N.

with N. $C_{(N,1),(N,N)}$ is higher because the transmission along the diagonal is stronger than in other directions, as shown in Fig. 3.

IV. CONCLUSIONS

In conclusion, we have presented a method to numerically and exactly calculate the dynamics of spin networks, in particular those without analytical solutions. We illustrate the method by simulating quantum state or entanglement transmission through a uniformly coupled two-dimensional square spin lattice in a one-excitation subspace. The numerically exact simulation demonstrates that the central symmetry plays a decisive role in obtaining high-fidelity state transmission. In comparison with the very few analytically solvable spin lattice models, the presented numerically exact simulation of quantum state dynamics, in particular in the single-excitation subspace, can help in the study of significant but nonanalytical spin lattice models, in particular in higher dimensions.

ACKNOWLEDGMENTS

This material is based upon work supported by the NSFC (Grant No. 11005099), Fundamental Research Funds for the Central Universities (Grant No. 201013037), the Basque Government (Grant No. IT472-10), and the Spanish MICINN (Projects No. FIS2009-12773-C02-02 and No. FIS2012-36673-C03-03).

[1] S. Bose, Phys. Rev. Lett. **91**, 207901 (2003); Contemp. Phys. **48**, 13 (2007).
[2] M. Christandl, N. Datta, A. Ekert, and A. J. Landahl, Phys. Rev. Lett. **92**, 187902 (2004).
[3] L. Campos Venuti, C. Degli Esposti Boschi, and M. Roncaglia, Phys. Rev. Lett. **99**, 060401 (2007).
[4] L.-A. Wu, A. Miranowicz, X. B. Wang, Y.-X. Liu, and F. Nori, Phys. Rev. A **80**, 012332 (2009).
[5] Z. M. Wang, C. Allen Bishop, M. S. Byrd, B. Shao, and J. Zou, Phys. Rev. A **80**, 022330 (2009); C. A. Bishop, Y.-C. Ou, Z.-M. Wang, and M. S. Byrd, *ibid.* **81**, 042313 (2010).
[6] T. J. G. Apollaro, L. Banchi, A. Cuccoli, R. Vaia, and P. Verrucchi, Phys. Rev. A **85**, 052319 (2012).
[7] A. Zwick and O. Osenda, J. Phys. A **44**, 105302 (2011).
[8] A. Zwick, G. A. Álvarez, J. Stolze, and O. Osenda, Phys. Rev. A **85**, 012318 (2012).
[9] Z.-M. Wang, R.-S. Ma, C. A. Bishop, and Y.-J. Gu, Phys. Rev. A **86**, 022330 (2012).
[10] Z.-M. Wang, L.-A. Wu, C. A. Bishop, Y.-J. Gu, and M. S. Byrd, arXiv:quant-ph/12106550.
[11] L.-A. Wu, Y.-X. Liu, and F. Nori, Phys. Rev. A **80**, 042315 (2009).
[12] B.-Q. Liu, L.-A. Wu, B. Shao, and J. Zou, Phys. Rev. A **85**, 042328 (2012).
[13] L.-A. Wu, M. S. Byrd, Z. D. Wang, and B. Shao, Phys. Rev. A **82**, 052339 (2010).
[14] D. L. Feder, Phys. Rev. Lett. **97**, 180502 (2006); H. Miki, S. Tsujimoto, L. Vinet, and A. Zhedanov, Phys. Rev. A **85**, 062306 (2012).
[15] V. Karimipour, M. S. Rad, and M. Asoudeh, Phys. Rev. A **85**, 010302(R) (2012).
[16] Z.-M. Wang and J.-Y. Gu, Commun. Theor. Phys. **58**, 835 (2012).
[17] Q. Xu, G. Sadiek, and S. Kais, Phys. Rev. A **83**, 062312 (2011).
[18] G. Sadiek, Q. Xu, and Sabre Kais, Phys. Rev. A **85**, 042313 (2012).
[19] D. Burgarth and S. Bose, Phys. Rev. A **71**, 052315 (2005).
[20] L.-A. Wu and H. Toki, Phys. Lett. B **407**, 207 (1997).